



# Simultaneous Raman-Rayleigh-LIF Measurements and Numerical Modeling Results of a Lifted $\text{H}_2/\text{N}_2$ Turbulent Jet Flame in a Vitiated Coflow

R. Cabra, J.Y. Chen, and R.W. Dibble  
University of California, Berkeley, Berkeley, California

Y. Hamano  
Ishikawajima-Harima Heavy Industries Company, Ltd., Tokyo, Japan

A.N. Karpetis and R.S. Barlow  
Sandia National Laboratories, Livermore, California

## The NASA STI Program Office . . . in Profile

Since its founding, NASA has been dedicated to the advancement of aeronautics and space science. The NASA Scientific and Technical Information (STI) Program Office plays a key part in helping NASA maintain this important role.

The NASA STI Program Office is operated by Langley Research Center, the Lead Center for NASA's scientific and technical information. The NASA STI Program Office provides access to the NASA STI Database, the largest collection of aeronautical and space science STI in the world. The Program Office is also NASA's institutional mechanism for disseminating the results of its research and development activities. These results are published by NASA in the NASA STI Report Series, which includes the following report types:

- **TECHNICAL PUBLICATION.** Reports of completed research or a major significant phase of research that present the results of NASA programs and include extensive data or theoretical analysis. Includes compilations of significant scientific and technical data and information deemed to be of continuing reference value. NASA's counterpart of peer-reviewed formal professional papers but has less stringent limitations on manuscript length and extent of graphic presentations.
- **TECHNICAL MEMORANDUM.** Scientific and technical findings that are preliminary or of specialized interest, e.g., quick release reports, working papers, and bibliographies that contain minimal annotation. Does not contain extensive analysis.
- **CONTRACTOR REPORT.** Scientific and technical findings by NASA-sponsored contractors and grantees.

- **CONFERENCE PUBLICATION.** Collected papers from scientific and technical conferences, symposia, seminars, or other meetings sponsored or cosponsored by NASA.
- **SPECIAL PUBLICATION.** Scientific, technical, or historical information from NASA programs, projects, and missions, often concerned with subjects having substantial public interest.
- **TECHNICAL TRANSLATION.** English-language translations of foreign scientific and technical material pertinent to NASA's mission.

Specialized services that complement the STI Program Office's diverse offerings include creating custom thesauri, building customized databases, organizing and publishing research results . . . even providing videos.

For more information about the NASA STI Program Office, see the following:

- Access the NASA STI Program Home Page at <http://www.sti.nasa.gov>
- E-mail your question via the Internet to [help@sti.nasa.gov](mailto:help@sti.nasa.gov)
- Fax your question to the NASA Access Help Desk at 301-621-0134
- Telephone the NASA Access Help Desk at 301-621-0390
- Write to:  
NASA Access Help Desk  
NASA Center for Aerospace Information  
7121 Standard Drive  
Hanover, MD 21076



# Simultaneous Raman-Rayleigh-LIF Measurements and Numerical Modeling Results of a Lifted $\text{H}_2/\text{N}_2$ Turbulent Jet Flame in a Vitiated Coflow

R. Cabra, J.Y. Chen, and R.W. Dibble  
University of California, Berkeley, Berkeley, California

Y. Hamano  
Ishikawajima-Harima Heavy Industries Company, Ltd., Tokyo, Japan

A.N. Karpetis and R.S. Barlow  
Sandia National Laboratories, Livermore, California

Prepared for the  
2001 Spring Joint Meeting  
sponsored by the U.S. Sections of The Combustion Institute  
Berkeley, California, March 26-28, 2001

Prepared under Grant NAG3-2103

National Aeronautics and  
Space Administration

Glenn Research Center

## Acknowledgments

The work presented here is part of a project supported by NASA Glenn Research Center, Contract number NAG3-2103. Work at Sandia was supported by the United States Department of Energy, Office of Basic Energy Sciences. In addition, Ishikawajima-Harima Heavy Industries Company, Ltd. (IHI), Tokyo, Japan, supported by Y. Hamano.

Trade names or manufacturers' names are used in this report for identification only. This usage does not constitute an official endorsement, either expressed or implied, by the National Aeronautics and Space Administration.

The Aerospace Propulsion and Power Program at NASA Glenn Research Center sponsored this work.

Available from

NASA Center for Aerospace Information  
7121 Standard Drive  
Hanover, MD 21076

National Technical Information Service  
5285 Port Royal Road  
Springfield, VA 22100

Available electronically at <http://gltrs.grc.nasa.gov>

# **Simultaneous Raman-Rayleigh-LIF Measurements and Numerical Modeling Results of a Lifted H<sub>2</sub>/N<sub>2</sub> Turbulent Jet Flame in a Vitiated Coflow**

R. Cabra, J.Y. Chen, and R.W. Dibble  
University of California, Berkeley  
Berkeley, California  
ricardo@newton.berkeley.edu

Y. Hamano  
Ishikawajima-Harima Heavy Industries Company, Ltd.  
Tokyo, Japan

A.N. Karpets and R.S. Barlow  
Sandia National Laboratories  
Livermore, California

## **ABSTRACT**

An experimental and numerical investigation is presented of a H<sub>2</sub>/N<sub>2</sub> turbulent jet flame burner that has a novel vitiated coflow. The vitiated coflow emulates the recirculation region of most combustors, such as gas turbines or furnaces. Additionally, since the vitiated gases are coflowing, the burner allows for exploration of recirculation chemistry without the corresponding fluid mechanics of recirculation. Thus the vitiated coflow burner design facilitates the development of chemical kinetic combustion models without the added complexity of recirculation fluid mechanics.

Scalar measurements are reported for a turbulent jet flame of H<sub>2</sub>/N<sub>2</sub> in a coflow of combustion products from a lean ( $\phi=0.25$ ) H<sub>2</sub>/Air flame. The combination of laser-induced fluorescence, Rayleigh scattering and Raman scattering is used to obtain simultaneous measurements of the temperature, major species, as well as OH and NO. Laminar flame calculations with multi-component diffusivity are presented and do not agree well with the experimental results. Laminar flame calculations with equal diffusivity do agree when the premixing and preheating that occurs prior to flame stabilization is accounted for in the boundary conditions. Also presented is an exploratory pdf model that predicts the flame's axial profiles fairly well, but does not accurately predict the lift-off height.

## **INTRODUCTION**

Advanced combustor designs employ the back mixing of hot combustion products with cool reactants in order to achieve flame stabilization and keep combustor size to a minimum. This important feature is absent in the widely studied simple jet flame issuing into a coflow of air. Attempts have been made to incorporate this recirculation with bluff body and swirl flames. The shortfall to these approaches is that the chemical kinetics and complex recirculation and wall interactions are strongly coupled.

The coaxial jet flame in a coflow of hot combustion products (vitiating coflow) simplifies the fluid dynamics by emulating the preheating and premixing of recirculation without the actual recirculation. As a result, the decoupled chemical kinetics can be modeled with more detailed chemical mechanisms. The design allows for intense turbulent mixing while maintaining a stable flame, thus providing the opportunity to examine turbulent mixing and combustion under the flow conditions typical of, or beyond, advanced combustors. Most importantly, the novel, open configuration of the vitiating coflow burner provides both optical access and well-defined boundary conditions, thus making it amenable to optical diagnostics and computational explorations. In addition, flameless oxidation ("FLOX") can easily be explored with this burner [Wüning & Wüning 1997, Plessing et al. 1998].

The principle objective of our research efforts is to characterize and model lifted jet flames of simple hydrocarbons ( $\text{CH}_4$ ). As an incremental step towards that goal, the current, relatively simple lifted hydrogen jet flame is examined. There have been several comprehensive studies of hydrogen jet flames that included experimental and numerical efforts [Barlow et al. 1994, 1996, Meier et al. 1996, Neuber et al. 1998, Chen et al. 1996]. Furthermore, there are at least three data sets [Brockhinke et al. 2000, Tacke et al. 1998, Cheng et al. 1992] that provide comprehensive information for lifted  $\text{H}_2$  flames in a coflow of air. The vitiating coflow provides a fairly small increment of complexity with benefits that can contribute to the understanding of turbulent combustion fundamentals of hydrogen and subsequently, simple hydrocarbons.

Multiscalar measurements, even with modest accuracy, constitute a useful test for combustion models [Warnatz et al. 1999]. This report focuses on the multiscalar measurements of a lifted  $\text{H}_2/\text{N}_2$  jet flame in a vitiating coflow. These results are compared to laminar flame calculations with equal diffusivity and full transport and an exploratory PDF model.

## **EXPERIMENTAL AND NUMERICAL METHODS**

The combustor consists of a central  $\text{H}_2/\text{N}_2$  jet and a vitiating coflow as shown in Figure 1. Note that the flames in Figure 1 are  $\text{CH}_4$  flames. The coflow consists of combustion products of a highly turbulent, lean premixed  $\text{H}_2/\text{Air}$  Flame. The coflow flame is stabilized on a perforated disk. In order to stabilize a highly turbulent flame, the blockage of the perforated plate should be 80-90%. The coflow must be highly turbulent, or have enough momentum so as not to collapse. A detailed design package has been prepared and is accessible over the World Wide Web [Cabra 2000].

The nozzle exit is high enough (7cm) above the perforated plate so that a uniform flow field can be assumed, based on the idea that the small-scale turbulence generated by a perforated plate is quickly dissipated. The temperature and oxygen level of the coflow can be adjusted; the operating range of the burner has previously been presented [Cabra et al. 2000].

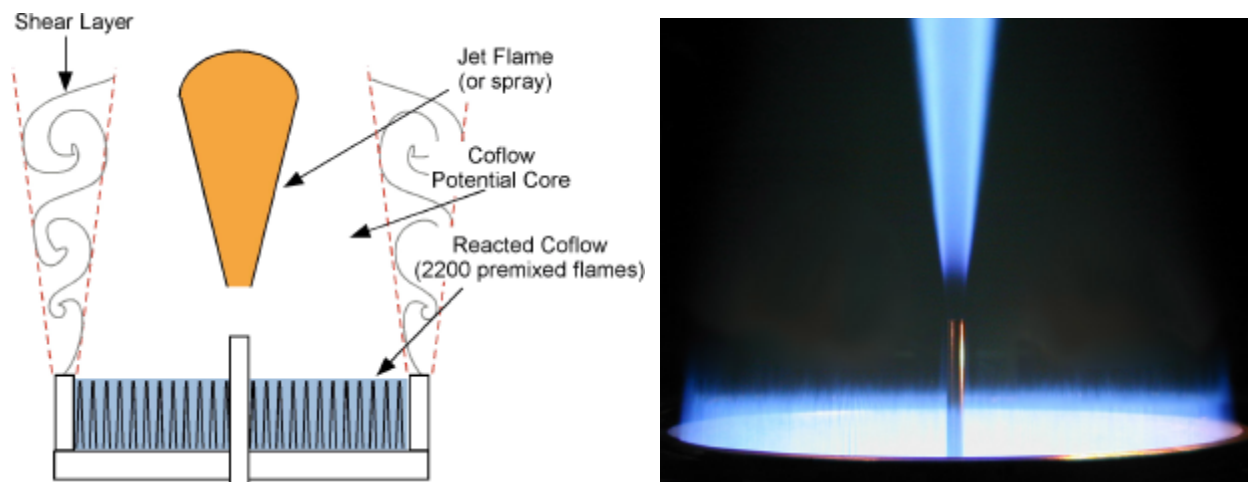


**Figure 1.**  
Vitiated coflow combustor schematic, and photo of CH<sub>4</sub>-Air Jet in a CH<sub>4</sub>-Air Coflow.

Experiments were conducted on one jet flame that consisted of 25% H<sub>2</sub> in N<sub>2</sub> by volume with a total flow rate of 100slm. The Reynolds number of the jet was 24,000. The coflow was products from a H<sub>2</sub>/Air premixed flame ( $\phi=0.25$ ) with a temperature of 1035K and a total flow rate of 2325slm. The height of the base of the lifted flame from the nozzle exit was approximately  $z/d=10$  and the height of the flame was  $z/d=30$ . These characteristics are similar to those reported by Tacke et al. 1998 on a lifted H<sub>2</sub>/N<sub>2</sub> jet of the same composition (25%/75%) with a similar Reynolds number of 17,000 but with a cool, slow moving coflow (0.2 m/s). More information on the geometry and the flow conditions are summarized in Table 1.

**Table 1.**  
Flame and Flow Conditions

Central Jet		Coflow	
Q <sub>H2</sub> (slm)	25	Q <sub>H2</sub> (slm)	225
Q <sub>N2</sub> (slm)	75	Q <sub>AIR</sub> (slm)	2100
Ma <sub>JET</sub>	0.3	$\phi$	0.25
T(K)	300	T (K)	1035
V <sub>JET</sub> (m/s)	101	V <sub>COFLOW</sub> (m/s)	3.5
Re <sub>JET</sub>	23,600	Re <sub>COFLOW</sub>	18,600
d <sub>JET</sub> (mm)	4.57	D <sub>COFLOW</sub> (cm)	21

### Simultaneous Raman-Rayleigh-LIF Measurements

Multiscalar experiments were conducted in the Turbulent Diffusion Flame (TDF) laboratory at Sandia's Combustion Research Facility. The temporally and spatially resolved simultaneous measurements of major species, minor species and temperature were made with Raman-Rayleigh scattering and laser induced fluorescence (LIF) techniques. The LIF systems measured the OH and NO, while the Raman-Rayleigh system measured the N<sub>2</sub>, O<sub>2</sub>, H<sub>2</sub>O, H<sub>2</sub> and

temperature. Details on the experimental setup and the calibration techniques are presented elsewhere [Smith et al. 1995, Nguyen et al. 1995, 1996, Barlow et al. 1988, 1996, Nooren 1998].

The system is setup to acquire data to produce joint statistics of the temperature and the major and minor species. The 5 lasers, (2 Raman-Rayleigh, 3 LIF) fire virtually simultaneously, with a delay of 100ns between shots. The laser pulse rate is 10 Hz. The spatial resolution of the system is 750 $\mu$ m.

The precision and accuracy of the Raman-Rayleigh-LIF system is determined with the use of flat calibration flames [Barlow et al. 2000]. The precision of single-shot measurements in a H<sub>2</sub> flame (no fluorescence interferences) is limited by the photoelectron shot noise [Dibble et al. 1987]. The accuracy of the equipment is ultimately determined by the calibration flame measurements. Figure 2 shows the measurements of a CH<sub>4</sub>/Air Hencken-burner taken prior to the H<sub>2</sub>/N<sub>2</sub> lifted flame experiment. The rms of the concentration or temperature and the mixture fraction data binds the ellipse that surrounds each point in Figure 2.

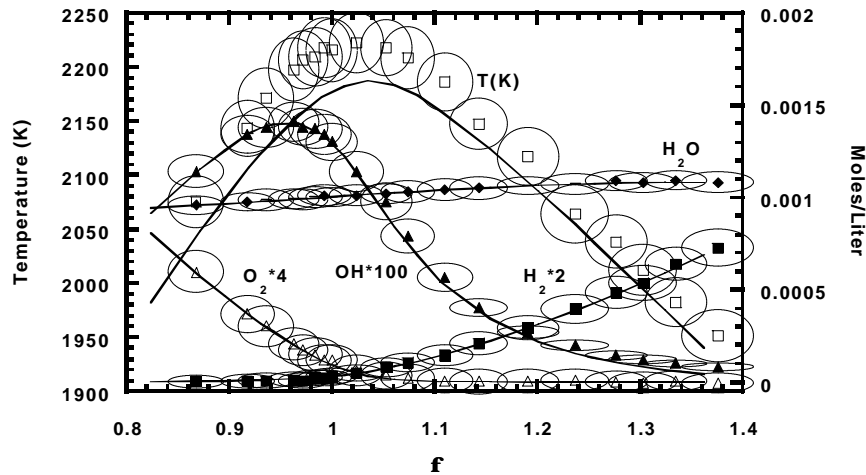


**Figure 2.**

Processed mean values of temperature and concentrations in the CH<sub>4</sub>-Air Hencken-burner flames.

### Probability Density Function Modelling Method

Joint probability density function (PDF) methods have been demonstrated to be useful in the modeling of turbulent combustion with local extinction. Utilized is the joint probability density function for composition only. Equation (1) shows the instantaneous transport and production of N reactive scalars  $\phi_i$ .

$$\rho \frac{\partial \phi_i}{\partial t} + \rho \nabla \cdot \phi_i = \nabla \cdot (\rho D \nabla \phi_i) + w_i(\phi_1, \dots, \phi_N) \quad (1)$$

The corresponding density-weighted PDF equation is:

$$\begin{aligned} & \langle \rho \rangle \frac{\partial \tilde{P}}{\partial t} + \langle \rho \rangle \tilde{\mathbf{y}} \cdot \nabla \tilde{P} + \langle \rho \rangle \sum_{i=1}^N \frac{\partial}{\partial \psi_i} \left( w_i(\psi_1, \dots, \psi_N) \tilde{P} \right) \\ & = -\nabla \cdot \left( \langle \rho \rangle \left\langle \tilde{\mathbf{y}}'' \middle| \phi_i = \psi_i \right\rangle \tilde{P} \right) - \langle \rho \rangle \sum_{i=1}^N \sum_{j=1}^N \frac{\partial^2}{\partial \psi_i \partial \psi_j} \left( \left\langle \epsilon_{ij} \middle| \phi_k = \psi_k \right\rangle \tilde{P} \right), \end{aligned} \quad (2)$$



where  $\psi_i$  are the sample space variables corresponding to the reactive scalars  $\phi_i$ ;  $\bar{v}$  and  $\bar{v}''$  denote the density weighted average velocity and its variance. In Equation (3)  $\epsilon_{ij}$  denotes the scalar dissipation rate defined as.

$$\epsilon_{ij} \equiv D \nabla \phi_i \cdot \nabla \phi_j \quad (3)$$

The turbulent flux and scalar dissipative terms appearing in the PDF transport equation are modeled. A gradient diffusion model is used for the turbulent flux and the Curl mixing model [Pope 1990] is used for the scalar dissipation rate.

The Monte Carlo simulation technique is used to compute the transport equation for the pdf [Chen & Kollmann 1988]. The Monte Carlo technique handles a collection of stochastic particles, involved in a simulation of convection, turbulent diffusion, molecular diffusion, and chemical reactions. The distribution of these stochastic particles in composition space then determines the form of the pdf. Subsequently, the single point statistics of the scalar variables  $\phi_i$  thru  $\phi_N$  are determined via  $\psi_i$  and the pdf. The computation power required by the multi-dimensional joint scalar pdfs limits the complexity of the reduced mechanisms for the combustion process. Currently, a 5-step reduced chemistry (4 steps for combustion and 1 step for thermal NO formation) is used for the modeling. In the reduced chemistry, both  $\text{HO}_2$  and  $\text{H}_2\text{O}_2$  are assumed to be in steady state, which may be relaxed in future modeling work.

## **RESULTS AND DISCUSSION**

The structure of the  $\text{H}_2/\text{N}_2$  lifted jet flame is measured by obtaining several radial profiles and an axial profile of temperature and species concentration. Figure 3 shows the points where measurements were taken. The region in the flame where flame stabilization occurs was of interest; therefore several points were measured in this region. The axial profile consists of measurements from  $z/d=1$  to  $z/d=34$  from the nozzle exit. Radial profiles were also obtained at several vertical distances ( $z/d = 1, 8, 9, 10, 11, 14$  &  $26$ ). The radial domain covered by these radial sweeps was -10mm to 50mm with step sizes typically between 1 and 3mm.

The single shot data has been processed and the Favre averages and conditional mean averages along with their respective rms fluctuations were calculated. A modified Bilger formulation [Bilger et al. 1990], with the carbon components omitted since there is no appreciable carbon in the system, determines the mixture fraction.

$$f_{\text{Bilger}} = \frac{\frac{1}{2M_H}(Y_H - Y_{H,2}) - \frac{1}{M_O}(Y_O - Y_{O,2})}{\frac{1}{2M_H}(Y_{H,1} - Y_{H,2}) - \frac{1}{M_O}(Y_{O,1} - Y_{O,2})} \quad (4)$$

Where  $Y$  is the elemental mass fraction and  $M$  is the atomic weight. Subscript 1 denotes the fuel stream and subscript 2 denotes the oxidizer stream. The elemental mass fractions at the boundary conditions are tabulated below in Table 2. The stoichiometric mixture fraction for these boundary conditions is  $f_s = 0.475$ .

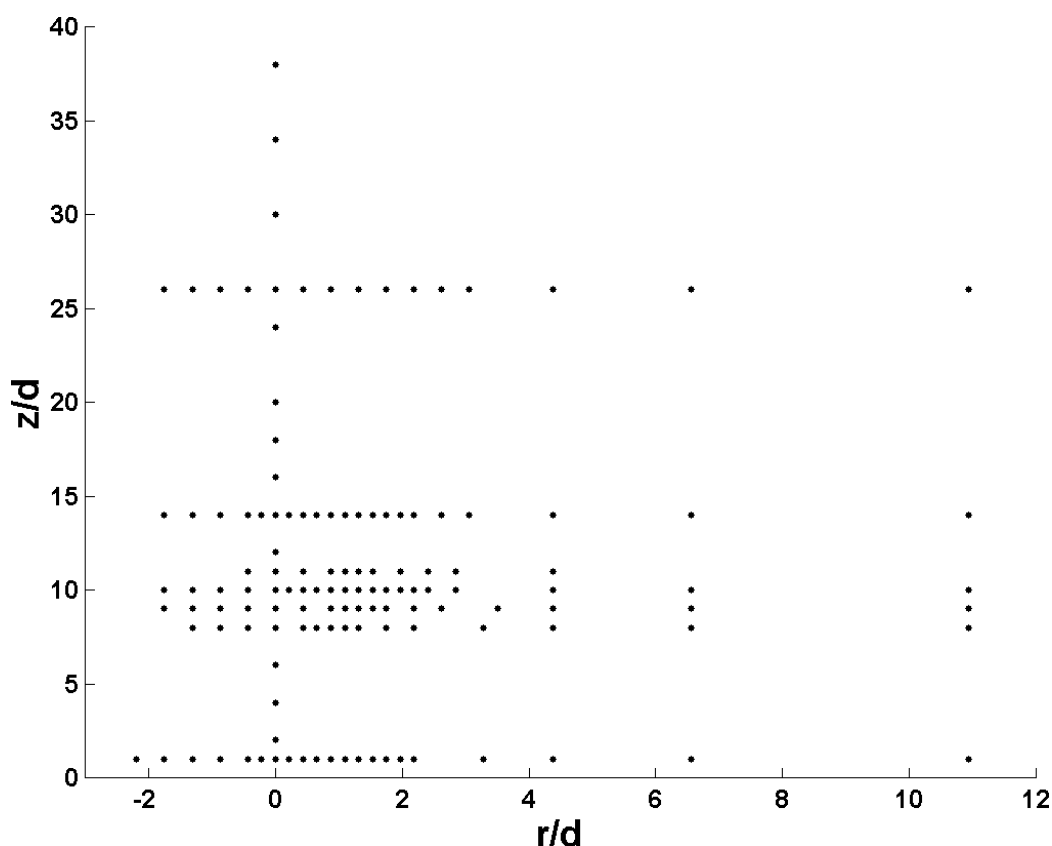


**Figure 3.**  
Location of measurement points (horizontal axis is expanded)

**Table 2.**  
Elemental mass fraction boundary conditions

Stream	$Y_H$	$Y_O$	$Y_N$
Fuel, 1	0.0237	0.0	0.9763
Coflow, 0	0.0074	0.2313	0.7613

### Radial and Axial Profiles

The radial profiles at  $z/d = 1, 14$  and  $26$  of Favre averaged temperature and species mole fractions are plotted in Figure 4. The radial profiles at  $z/d = 8, 9, 10$  and  $11$  are included as an appendix. Two important design benefits are demonstrated in Figure 4. First, relatively flat profiles at  $z/d=1$  show that the boundary conditions are well defined. Second, the integrity of the coflow is undiminished as temperature and species measurements in the far field remain steady throughout the range of measurements in the vertical direction.

Axial profiles of the Favre averaged temperature, mixture fraction and specie mole fractions are plotted in Figure 5. The results from the PDF model are also plotted with the experimental data. Two PDF model simulations were conducted, for both a reacting and non-reacting (pure mixing) flow. The solid lines indicate the reacting case and the dashed lines denote the non-reacting case.

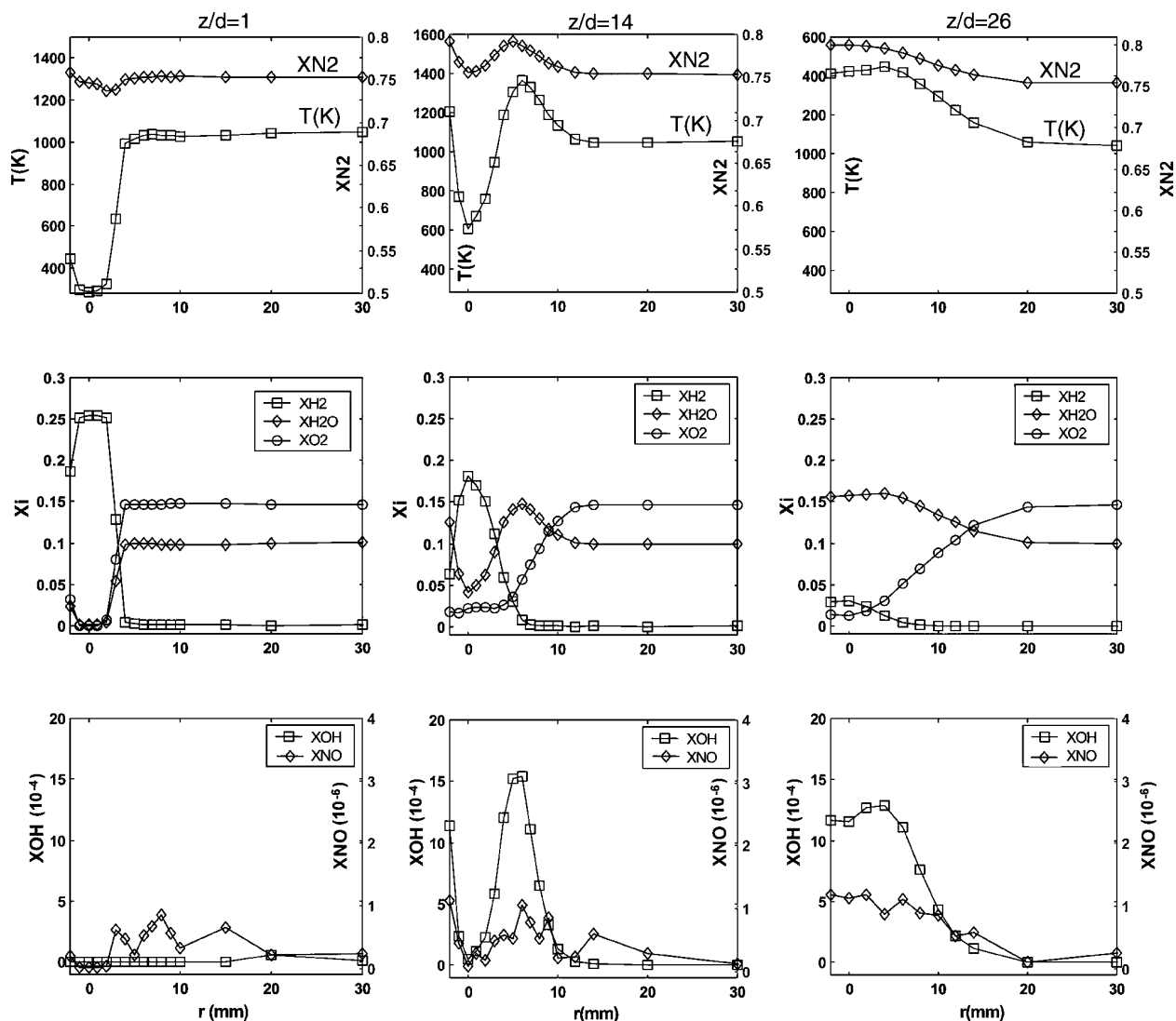


**Figure 4.**

Radial profiles of Favre averages for temperature and specie concentrations at axial locations  $z/d=1$  (left column),  $z/d=14$  (central column) and  $z/d=26$  (right column).

Lifted flames exhibit characteristics similar to both reactive and non-reactive flows, with the transition occurring at the base of the flame. The flame front acts as a barrier, limiting the mixing of the two streams. Therefore, as in the case of the mixture fraction, the non-reacting case exhibits steep gradients in the  $z$ -direction, in contrast to the more gradual trend in the reacting case. After the potential core is dissipated, the experimental results show this pure mixing and preheat in the region between the nozzle exit and the base of the flame. At the onset of combustion at the axis ( $z/d=13$ ) the experimental results then demonstrate the limited mixing caused by the flame, the production of combustion products  $H_2O$ ,  $OH$  and  $NO$  and increase in temperature. However, the model predicts an accelerated ignition time, as can be seen in the temperature and  $OH$  mole fraction plots, this reduces the amount of mixing and entrainment of the coflow and central jet.

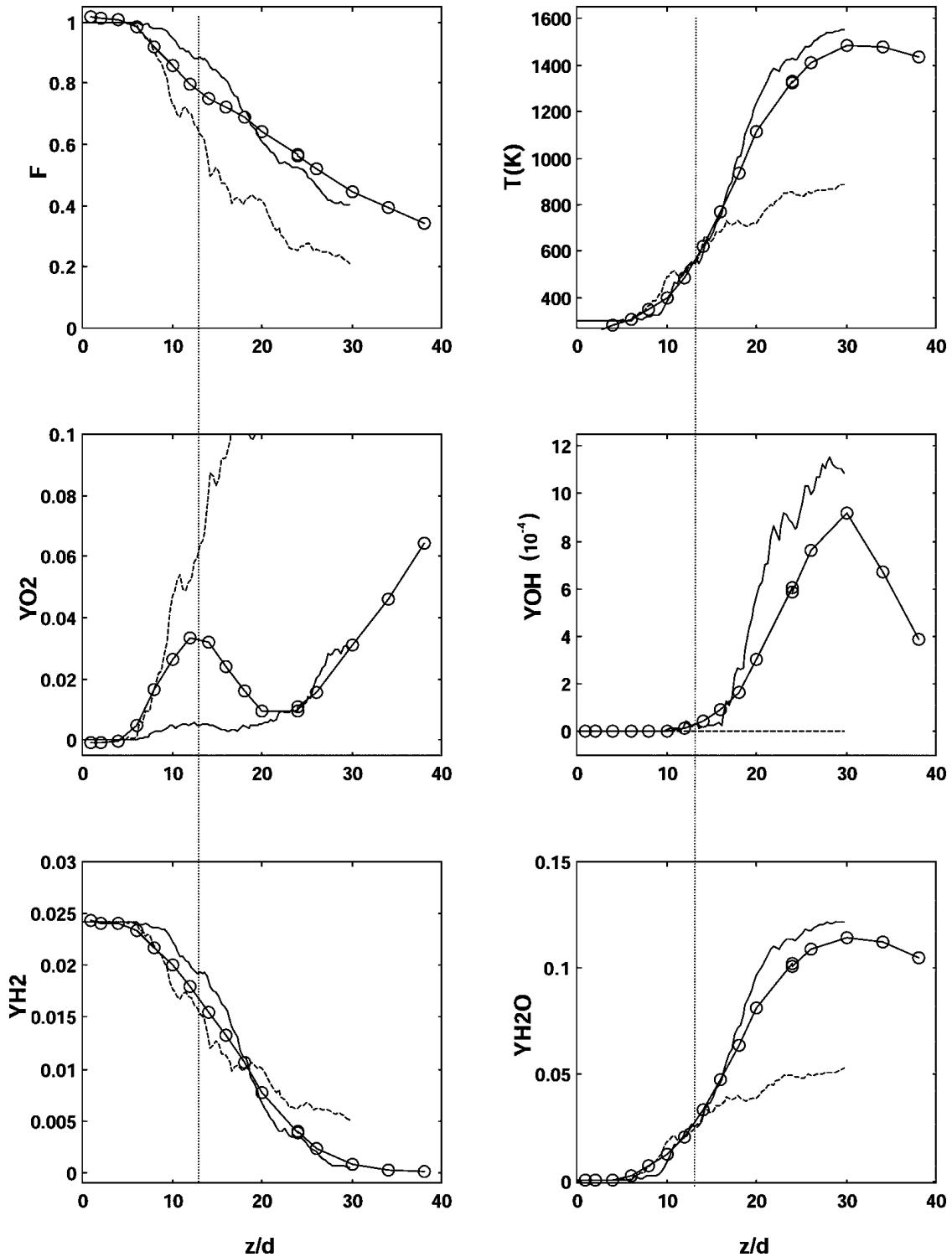


**Figure 5.**

Axial profiles of the Favre average and rms fluctuation compared with the PDF model results. The connected circles are the experimental results. The reacting flow is plotted with solid lines while the non-reacting flow is plotted with dashed lines. The vertical dotted lines mark the onset of combustion at the axis ( $z/d=13$ ).

The hot oxidizer is entrained and preheats the fuel stream. The oxygen mass fraction reaches a maximum at approximately  $z/d=3$  where the temperature is  $\approx 550\text{K}$  and the mixture fraction is  $\approx 0.8$ .

The aggregate experimental results of the radial profiles were used to generate a low-resolution color map of the temperature and species concentrations. The axial profile data was excluded from this process since it produced a significant bias for gradients in the radial direction. There is good resolution in the area where the flame stabilization occurs since several points were measured in this region. The temperature and OH color maps for the aggregate experimental data, and the results from the PDF model are plotted in Figure 6. Note the different YOH scales for the PDF and experimental results.

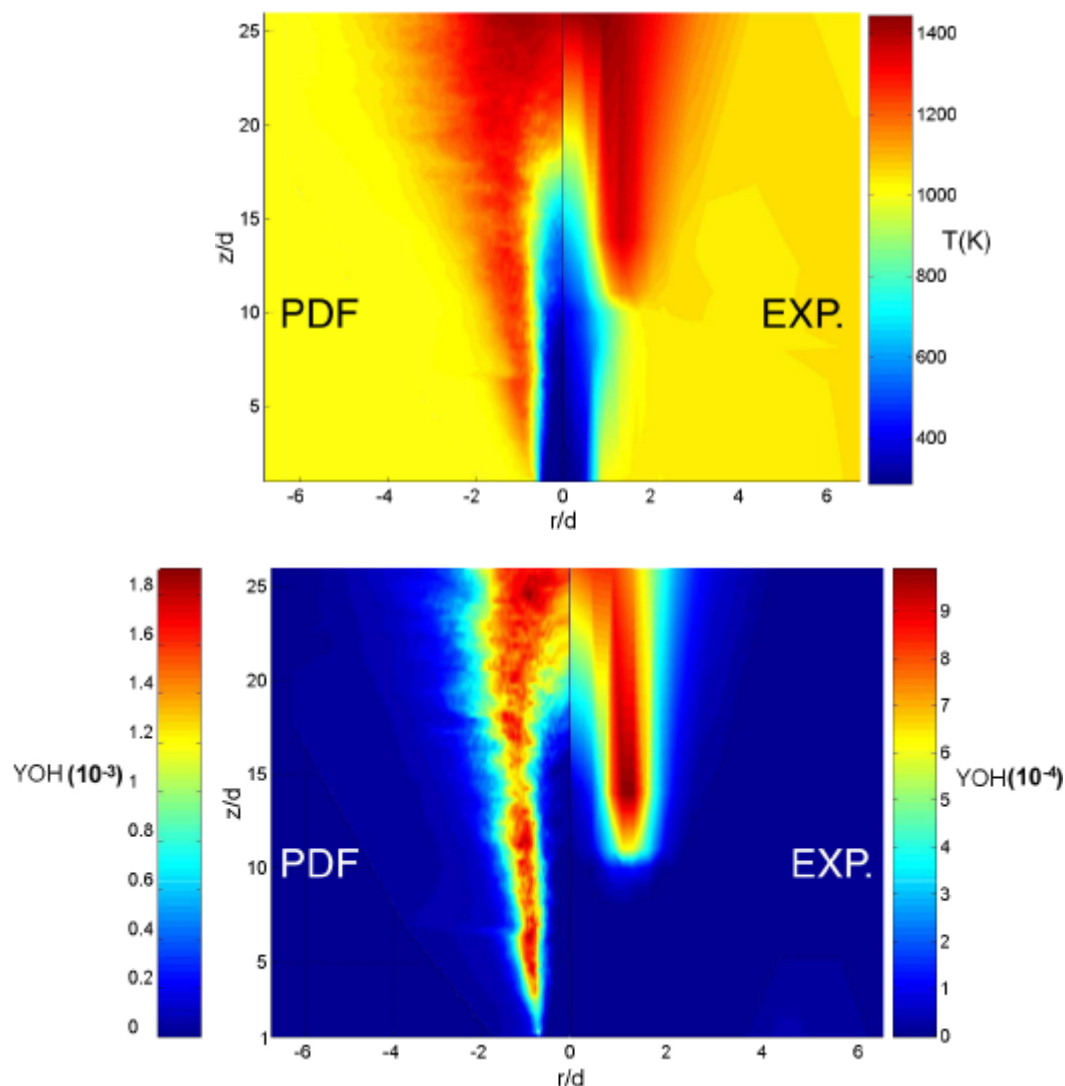


**Figure 6.**

Experimental and PDF color maps of temperature (top) and YOH (bottom). Note the different YOH scales for the PDF and experimental results.

Comparisons between the experimental and numerical results show that the numerical model does not accurately predict flame lift off. Sudden spatial increases in OH levels mark the flame edge [Tacke 1998]. For our purposes here, we define the flame as the zone where the OH mole fraction is greater than  $6 \times 10^{-4}$ . The experimental flame stabilization height is approximately  $H_{EXP}/d=10$  and the model predicts  $H_{PDF}/d=2$ . Likewise, the radius of the base of the flame is  $R_S/d=1.5$  and the model predicts  $R_{PDF}/d=0.75$ . The levels of YOH in the experiment are approximately 50% of those predicted by the model. Above the stabilization point, the experiment and model agree.

A reason for the difference in results between the experiment and the model is that the boundary conditions were slightly different. The raw experimental data goes through an iterative reduction process and preliminary experimental results were inadvertently used as boundary conditions for the PDF model. The differences between the experiment and model boundary conditions are listed in Table 3. These differences in the boundary conditions (2-3%) can have a substantial effect on the flame, therefore the PDF model must be modified and rerun.

**Table 3.**  
Differences in preliminary and final experimental results

	Model	Experiment	Calculated*
<b><u>Jet</u></b>			
Temperature (K)	295	291	300
XH <sub>2</sub>	0.254	0.254	0.252
XN <sub>2</sub>	0.737	0.746	0.748
<b><u>Coflow</u></b>			
Temperature (K)	1070	1035	1080
XO <sub>2</sub>	0.15	0.147	0.148
XH <sub>2</sub> O	0.102	0.099	0.102
XN <sub>2</sub>	0.746	0.753	0.749

\* The calculated values are based on mass flow controller readings and equilibrium calculations.

### Conditional Statistics and Issues of Scalar Transport

The central fuel jet entrains hot products from the coflow, thus evolving into a preheated, partially premixed flow prior to the onset of combustion. The Favre averaged measurements presented in the previous section show the entrainment of oxidizer into the fuel stream prior to combustion, thus further diverging the combustion statistics of this flame from those of a system at equilibrium. The scatter data of the temperature and oxygen mass fraction are presented in Figure 7. The data plotted in Figure 7 is a composite of the single shot data from the radial profile at  $z/d=14$ . Approximately 6000 data points are plotted. The partially premixed nature of the flame is shown by the penetration of oxygen to the rich mixture fraction space.

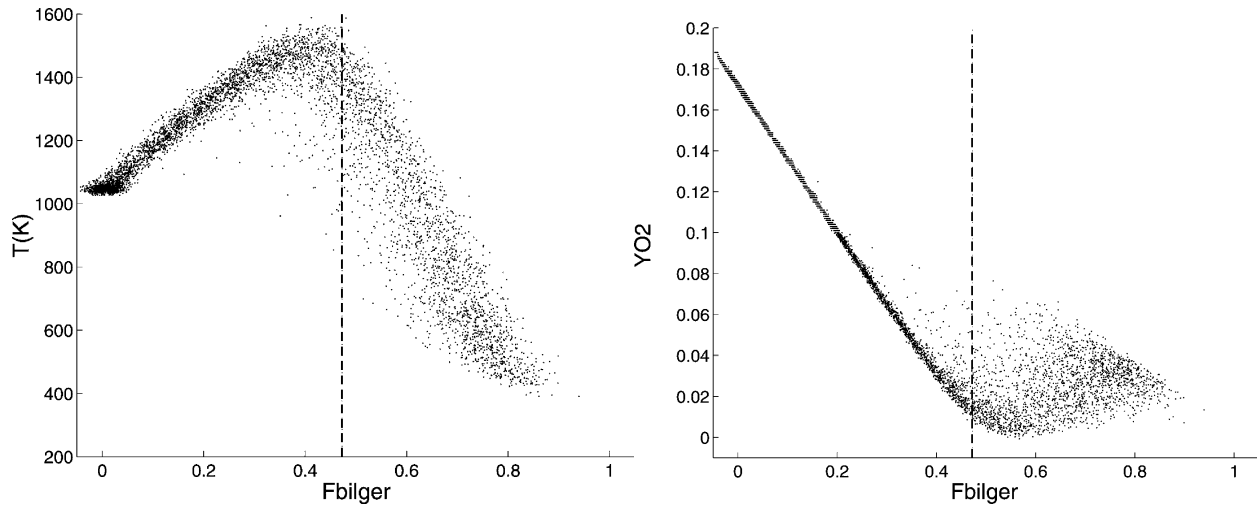


**Figure 7.**

Scatter plot of single-shot temperature and  $YO_2$  measurements at  $z/d = 14$ . The number of data points is approximately 6,000. The vertical dotted line indicates the stoichiometric value of the mixture fraction.

The conditional means with the conditional rms ( $\pm\sigma$ ) fluctuations plotted as error bars for the temperature and oxygen mass fraction corresponding to the scatter data in Figure 7 is plotted in Figure 8. The conditional means and rms are calculated at constant intervals of  $\Delta f = 0.02$ . Equilibrium calculation results are also plotted as solid lines.

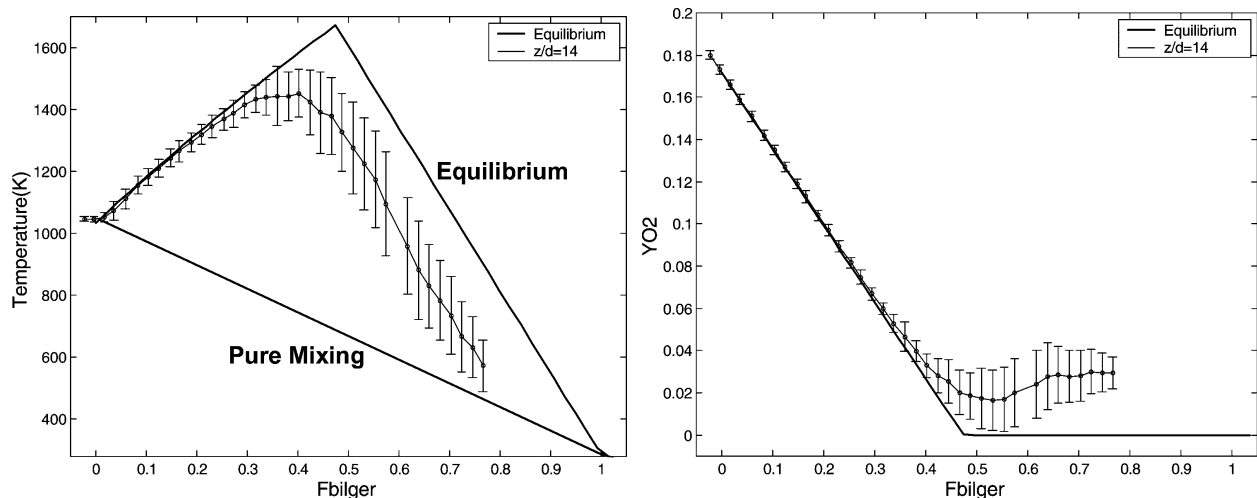


**Figure 8.**

Conditional means and rms fluctuations plotted as uncertainty bars. The solid line is the results of equilibrium calculations of the fuel and oxidizer.

Tsuji opposed flow laminar flame calculations were made with full molecular transport and equal molecular and thermal diffusivities. The results from the calculations with full molecular transport are plotted in Figure 9 along with the conditional means and rms fluctuations for  $z/d = 14$ .

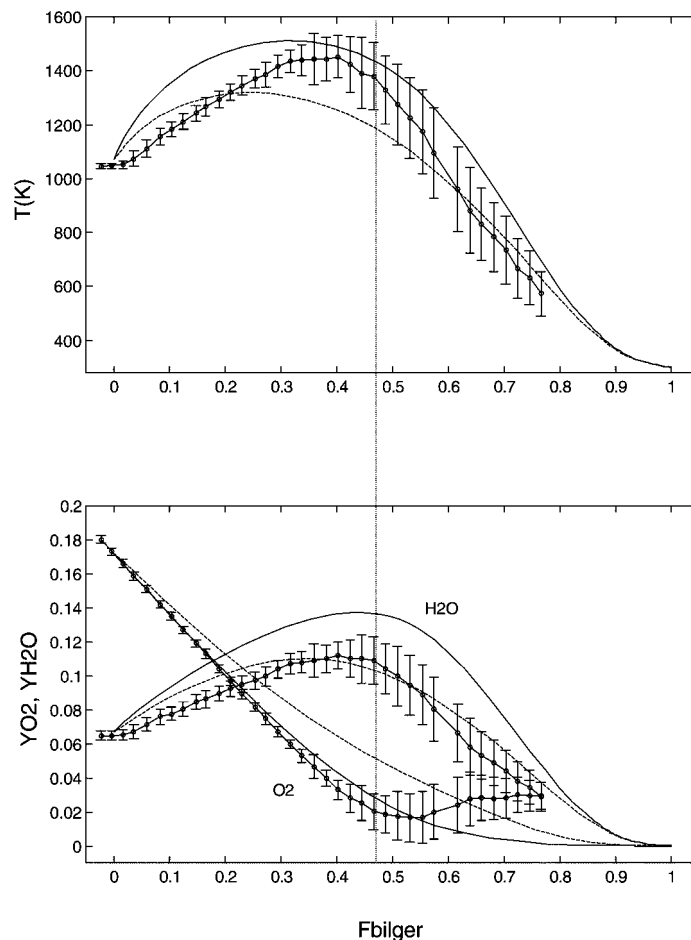


**Figure 9.**

Results of steady strained opposed-flow laminar flame calculations with full molecular transport. Conditional means and rms fluctuations (error bars) of temperature,  $\text{H}_2\text{O}$  and  $\text{O}_2$  mass fractions are plotted against laminar flame calculations with strain rates of  $a=8,000$   $1/s$  (solid lines) and  $a=20,000$   $1/s$  (dashed lines). The vertical dotted line indicates the stoichiometric mixture fraction.

There are considerable discrepancies between the full molecular transport calculations and the experimental results. This is in agreement with the well-documented findings of Barlow et al. 1996 & 2000. The mixture fraction domain over which reactions occur is smaller than what the calculations predict. This shows that the turbulent mode of mixing may be dominant. Therefore, the calculations were rerun with equal diffusivities.

The presence of oxidizer in the fuel stream is evident in the mixing line that diverges from the equilibrium curve in the rich mixture fraction space (Figure 8). Since the flame is lifted, the fuel stream becomes partially premixed, thus changing the effective boundary conditions for the opposed flow flames calculations. For the equal diffusivity calculations, the fuel side boundary condition was set to  $f \approx 0.8$  which is approximately the mixture fraction corresponding to the onset of combustion as presented in the axial profiles ( $z/d=13$ ). The temperature is approximated to be 440K, the temperature corresponding to  $f=0.8$  on the pure-mixing line in Figure 8. The results of these calculations are plotted in Figure 10.



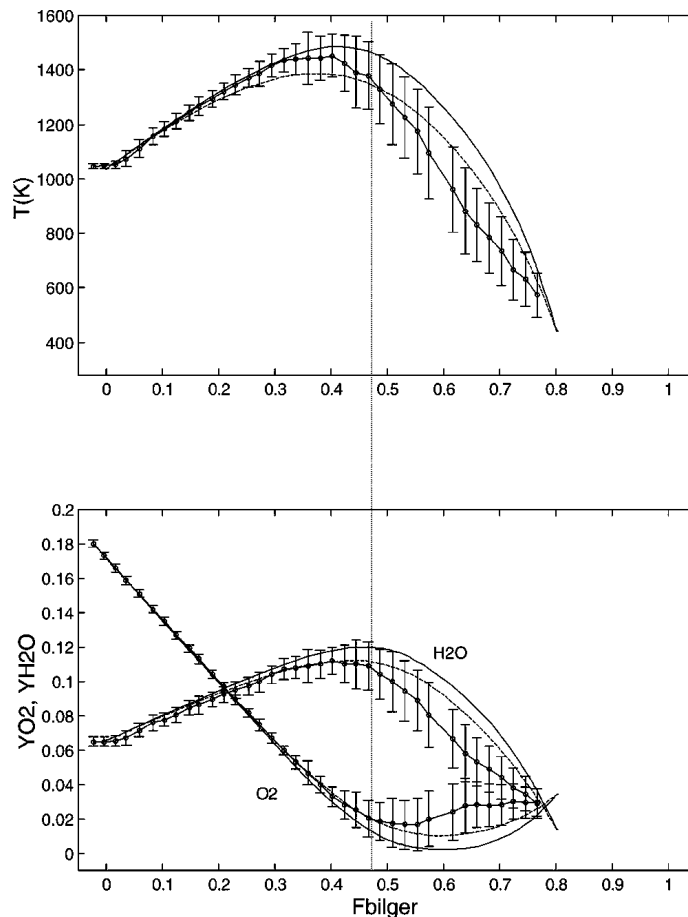


**Figure 10.**

Results of steady strained opposed-flow laminar flame calculations with equal specie and thermal diffusivities. Conditional means and rms fluctuations (error bars) of temperature,  $\text{H}_2\text{O}$  and  $\text{O}_2$  mass fractions are plotted against laminar flame calculations with strain rates of  $a=1,000$   $1/\text{s}$  (solid lines) and  $a=4,000$   $1/\text{s}$  (dashed lines). The vertical dotted line indicates the stoichiometric mixture fraction.

There is good agreement between the experimental and equal diffusion calculations. The contrast of this agreement with that of the experimental and full transport calculations suggests that turbulent transport is dominant over molecular transport. There is some discrepancy on the rich mixture fraction space. This may be due to the heat loss to the combustor in the opposed flow flame calculations. Future calculations will be performed to see if better agreement can be achieved by a more adiabatic system with increased flow velocity with constant strain rate.

## **CONCLUSIONS:**

Simultaneous multiscalar measurements of a lifted  $\text{H}_2/\text{N}_2$  jet have been presented and provide the basis for insight into flame structure of a lifted flame. The flame exhibits the partial premixing inherent in lifted-off flames, while also being preheated by the entrained hot coflow.

Laminar flow calculations with full molecular transport have also been made and do not agree well with the experimental results. However, the laminar flame calculations with equal diffusivities agree well when the preheating and premixing in the jet prior to the flame stabilization is accounted for in the boundary conditions. An exploratory PDF simulation of the system has been conducted and has been presented. It does model the axial profiles somewhat accurately, but it does not model the lift-off height.

## **REFERENCES**

- Barlow, R.S., Fiechtner, G.J., Carter, C.D., & Chen, J.-Y., *Combust. Flame* **120**:549-569 (2000)
- Barlow, R.S., & Carter, C.D., *Combust. Flame* **97**:261-280 (1994)
- Barlow, R.S., & Carter, C.D., *Combust. Flame* **104**:288-299 (1996)
- Barlow, R.S., Dibble, R.W., Chen, J.-Y. & Lucht, R.P., *Combust. Flame* **82**, 235 (1988).
- Barlow, R.S., Fiechtner, G.J., & Chen, J.-Y., *Twenty-Sixth Symposium (International) on Combustion, The Combustion Institute, Pittsburgh, PA*, pp. 2199-2205 (1996)
- Bilger, R.W., Ståner, S.H., & Kee, R.J., *Combust. Flame* **80**:135-149 (1990)
- Brockhinke A., Haufe, S. & Kohse-Höinghaus, *Combust. Flame* **121**:367-377 (2000)
- Cabra R., *Vitiated Coflow Combustor Design Pak* <http://www.me.berkeley/cal/vcb> (2000)
- Cabra R. Hamano, Y., Chen, J.-Y., Dibble, R.W., Acosta, F. & Holve, D. *Spring Meeting of the Western States Section of the Combustion Institute, Golden, CO*, WSS/CI 00S-47 (2000)
- Chen, J.-Y. & Kollmann W., *Twenty-Second Symposium (International) on Combustion, the Combustion Institute*, pp. 645-653 (1988)
- Chen, J.-Y., Chang, Y.-C., & Koszykowski, M., *Comb. Sci. Tech.* **110**:505 (1996)
- Cheng, T.S., Wehrmeyer, J.A., & Pitz, R.W., *Combust. Flame*, **91**:323-345 (1992)
- Dibble, R.W., Masri, A.R., & Bilger, R.W., *Combust. Flame*, **67**:167 (1987)
- Meier, W., Vydorov, A.O., Bergmann, V., & Stricker, W., *Appl. Phys. B* **63**:79-90 (1996)
- Neuber, A., Krieger, G., Tacke, M., Hassel, E.P., & Janicka, J., *Combust. Flame* **113**:198-211 (1998)
- Nguyen, Q.V., Dibble, R.W., Carter, C.D., Fiechtner, G.J., & Barlow, R.S., *Combust. Flame* **105**:499-510 (1996).
- Nguyen, Q.V., Ph.D. Thesis for UC Berkeley (1995)
- Nooren, P., Ph.D. Thesis for T.U. Delft (1998)
- Pope, S.B., *Twenty-Third Symposium (International) on Combustion*, pp. 591-612 (1990)
- Smith N.S.A., Bilger, R.W., Carter, C.D., Barlow R.S., & Chen, J.Y., *Comb. Sci. and Tech.*, **105**:357-375 (1995).
- Tacke, M.M., Geyer, D., Hassel, E.P., & Janicka J., *Twenty-Third Symposium (International) on Combustion*, pp. 1157-1165 (1998)
- Warnatz, J., Maas, U., & Dibble, R.W., *Combustion: Physical and Chemical Fundamentals, Modeling and Simulation, Experiments, Pollutant Formation, 2<sup>nd</sup> Ed.*, Springer-Verlag (1999)

# APPENDIX

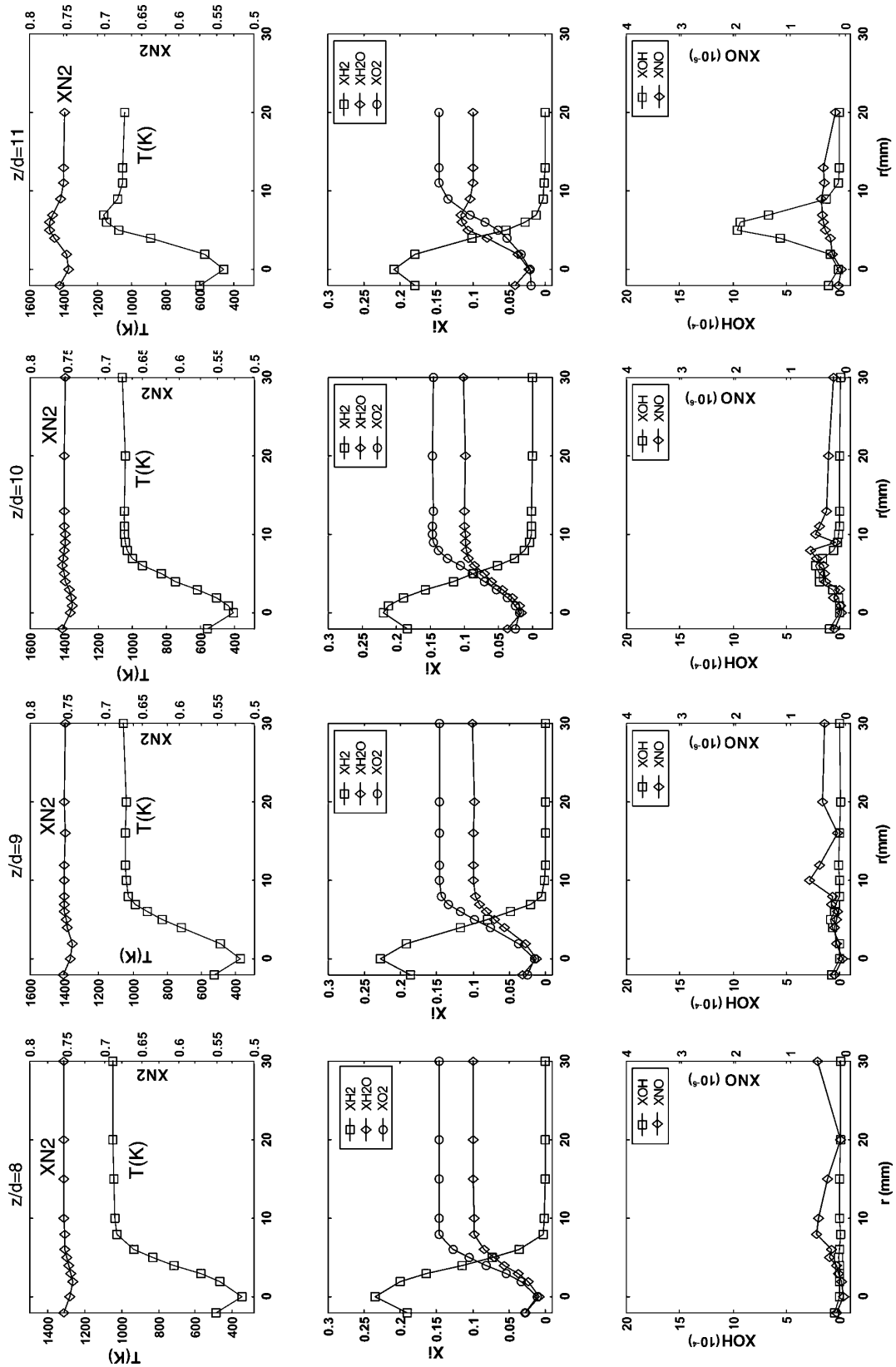


**Figure 10.** Radial profiles of Favre averages for temperature and species concentrations at axial locations  $z/d=8, 9, 10$  and  $11$ .

REPORT DOCUMENTATION PAGE			Form Approved OMB No. 0704-0188	
Public reporting burden for this collection of information is estimated to average 1 hour per response, including the time for reviewing instructions, searching existing data sources, gathering and maintaining the data needed, and completing and reviewing the collection of information. Send comments regarding this burden estimate or any other aspect of this collection of information, including suggestions for reducing this burden, to Washington Headquarters Services, Directorate for Information Operations and Reports, 1215 Jefferson Davis Highway, Suite 1204, Arlington, VA 22202-4302, and to the Office of Management and Budget, Paperwork Reduction Project (0704-0188), Washington, DC 20503.				
1. AGENCY USE ONLY (Leave blank)		2. REPORT DATE December 2002		3. REPORT TYPE AND DATES COVERED Final Contractor Report
4. TITLE AND SUBTITLE  Simultaneous Raman-Rayleigh-LIF Measurements and Numerical Modeling Results of a Lifted H <sub>2</sub> /N <sub>2</sub> Turbulent Jet Flame in a Vitiated Coflow			5. FUNDING NUMBERS  WBS-22-708-90-01 NAG3-2103	
6. AUTHOR(S)  R. Cabra, J.Y. Chen, R.W. Dibble, Y. Hamano, A.N. Karpets, and R.S. Barlow				
7. PERFORMING ORGANIZATION NAME(S) AND ADDRESS(ES)  University of California, Berkeley Berkeley, California 94720			8. PERFORMING ORGANIZATION REPORT NUMBER  E-13734	
9. SPONSORING/MONITORING AGENCY NAME(S) AND ADDRESS(ES)  National Aeronautics and Space Administration Washington, DC 20546-0001			10. SPONSORING/MONITORING AGENCY REPORT NUMBER  NASA CR-2002-212081	
11. SUPPLEMENTARY NOTES Prepared for the 2001 Spring Joint Meeting sponsored by the U.S. Sections of The Combustion Institute, Berkeley, California, March 26-28, 2001. R. Cabra, J.Y. Chen and R.W. Dibble, University of California, Berkeley, Berkeley, California 94720; Y. Hamano, Ishikawajima-Harima Heavy Industries Company, Ltd. (IHI), Tokyo, Japan; A.N. Karpets and R.S. Barlow, Sandia National Laboratories, Livermore, California 94551. Project Manager, James D. Holdeman, Turbomachinery and Propulsion Systems Division, NASA Glenn Research Center, organization code 5830, 216-433-5846.				
12a. DISTRIBUTION/AVAILABILITY STATEMENT  Unclassified - Unlimited Subject Category: 07  Available electronically at <a href="http://gltrs.grc.nasa.gov">http://gltrs.grc.nasa.gov</a> This publication is available from the NASA Center for AeroSpace Information, 301-621-0390.			12b. DISTRIBUTION CODE	
13. ABSTRACT (Maximum 200 words)  An experimental and numerical investigation is presented of a H <sub>2</sub> /N <sub>2</sub> turbulent jet flame burner that has a novel vitiated coflow. The vitiated coflow emulates the recirculation region of most combustors, such as gas turbines or furnaces. Additionally, since the vitiated gases are coflowing, the burner allows for exploration of recirculation chemistry without the corresponding fluid mechanics of recirculation. Thus the vitiated coflow burner design facilitates the development of chemical kinetic combustion models without the added complexity of recirculation fluid mechanics. Scalar measurements are reported for a turbulent jet flame of H <sub>2</sub> /N <sub>2</sub> in a coflow of combustion products from a lean ( $\phi = 0.25$ ) H <sub>2</sub> /Air flame. The combination of laser-induced fluorescence, Rayleigh scattering, and Raman scattering is used to obtain simultaneous measurements of the temperature, major species, as well as OH and NO. Laminar flame calculation with equal diffusivity do agree when the premixing and preheating that occurs prior to flame stabilization is accounted for in the boundary conditions. Also presented is an exploratory pdf model that predicts the flame's axial profiles fairly well, but does not accurately predict the lift-off height.				
14. SUBJECT TERMS  Fuel spray; Combustion chamber; Gas turbines; Flames; Burners; Liquid fuels; Methyl alcohol; Raman spectroscopy; Laser induced fluorescence numerical analysis			15. NUMBER OF PAGES 21	
			16. PRICE CODE	
17. SECURITY CLASSIFICATION OF REPORT Unclassified	18. SECURITY CLASSIFICATION OF THIS PAGE Unclassified	19. SECURITY CLASSIFICATION OF ABSTRACT Unclassified	20. LIMITATION OF ABSTRACT	